Electron Temperature of Argon Pinch Produced by Microsecond Implosion of a Multishell Gas Puff

S.A. Chaikovsky, N.A. Zhidkova, A.V. Fedunin, A.Yu. Labetsky, V.A. Kokshenev,
V.I. Oreshkin, A.G. Rousskikh, A.V. Shishlov

Institute of High Current Electronics, 4 Akademichesky Ave., Tomsk, 634055, Russia,
3822-492-133, 3822-491-677, stas@ovpe.hcei.tsc.ru

Abstract – The experiments with an argon multiple shell gas puff z-pinch at microsecond implosion times were performed on the GIT-12 generator. The implosion dynamics was inferred from current and load voltage traces. Plasma electron temperature was measured by a ratio of x-ray detector responses. The results are discussed from viewpoint of argon K-shell production at a microsecond implosion time regime.

1. Introduction

Bright K-shell ($h\nu \geq 1$ keV) plasma radiation sources are conventionally based on a z-pinch implosion driven by a fast ($\tau \approx 100$ ns) pulsed power generator [1]. Slower generators, for example, a microsecond capacitor bank, potentially have lower cost, less technical complexity and high efficiency of conversion of the stored energy to the plasma kinetic energy. However, on such generators a large initial radius $r_0 > 4$ cm should be exploited in order to provide a specific energy per ion K_i [2] sufficient to ionize plasma into K-shell and excite the K-shell electrons. Some experimental and theoretical results (see, for example, [3, 4, 5, 6]) have shown that the high initial radius implosions are strongly affected by Rayleigh-Taylor (RT) instabilities. The instabilities can result in plasma sheath break up in the course of implosion that prevents a tight plasma pinch formation in the final implosion stage and efficient K-shell radiation production.

Tight plasma pinches could be produced and essentially better radiation performance could be attained using a staged z-pinch such as a double shell [7] or multiple shell [8] z-pinch. The neon K-shell yield observed on a microsecond capacitor bank with a double z-pinch can reach the typical neon K-shell yield values for a fast generator [9].

The paper presents results of experiments on argon K-shell ($h\nu \approx 3\div4$ keV) radiation production, which were performed on the GIT-12 pulse generator operating in a microsecond mode. The experiments were carried out with argon multi-shell gas puffs (shell-on-shell-on-solid-fill)) with the length of 1.8 cm. Two concentric annular gas jets had diameters of 16 cm (outer shell) and 8 cm (middle shell). The inner on-axis solid fill had the diameter of 2.2 cm. The load scheme, experimental results on K-shell yield and implosion stability can be found in accompanied papers [10, 11]. This paper concentrates on plasma temperature measurements and comparison of snowplow calculated implosion dynamics with experimental one.

2. Motivation of the Nozzle Parameter Choice

The GIT-12 generator was redesigned for direct drive microsecond implosion experiments. In this mode the generator delivers 4.7 MA current with a rise time of 1.6 μs on a short-circuit load. The GIT-12 installation is composed of 12 modules and a central collector with a load unit. Each module consists of nine parallel Marx generators, a vacuum insulator, a vacuum coaxial line connecting the module to the central collector.

The implosion time was chosen to be close to 1 μs, since microsecond implosion experiments on K-shell radiation production was the point of interest.

The outer shell initial diameter was chosen to be 16 cm. According to snowplow calculations, this allows reaching a specific energy per argon ion $K_i \approx E_{min} = 38$ keV/ion [2] at the implosion time of $0.7\div0.9$ μs for reasonable ratios of the shell masses. The energy E_{min} is an energy per ion required to ionize argon atoms up to the K-shell and to heat the electrons up to the optimum K-shell emission temperature [2]. This approach assumes that conversion of the kinetic energy to plasma thermal energy in the final stage of implosion is the only mechanism responsible for plasma heating. Of course, it is preferable to have the energy K_i higher than E_{min} in order to have some energy reserve for radiation production. A number of experiments with single shell z-pinches have shown that the highest K-shell yield was observed at $K_i \approx (1.1\div1.4)\, E_{min}$ [12, 13] when the experimental conditions correspond to I^4 K-shell radiation scaling.

The middle and inner shell diameters were chosen to be approximately the same as in the experiments with a double shell z-pinch on the GIT-12, performed with a plasma opening switch at current rise time of 300 ns [14]. The middle shell diameter was 8 cm, while the inner shell was a solid fill with the outer diameter of 2.2 cm.

The reasons of such choice of the shell initial diameters were based on two opposite points of view. These viewpoints are not evidently true and introduce a number of simplifying assumptions. The first assumption is that the outer shell, which is surely affected by Rayleigh-Taylor instabilities, could be

stabilized by a middle shell due to snowplow stabilization [15, 16]. Further in the course of implosion the plasma sheath composed of the outer and middle shell could be stabilized by the inner shell. In this case the implosion dynamics should be described well by a snowplow model.

It seems to be reasonable to place a middle shell just on a half way of the outer shell. Such configuration allows reduction both the outer shell path (i.e. traveled distance) and the joined outer and middle sheath path. The reduction of the sheath path should decrease the instability level in the sheath. For example, in the linear approximation the e-folding number of RT instabilities $\Gamma \propto \int g^{0.5} dt \propto g^{0.5} \tau \propto s^{0.5}$, i.e. the shorter is the shell pass s, the lower is the instabilities level (here g – acceleration of the shell, τ – implosion time). Moreover, the amplitude of perturbation ξ seems to be proportional to the traveled distance in the nonlinear stage of the RT instability: $\xi \propto gt^2 \propto s$ (see, for example, [17]).

Another point of view takes into account a possibility of current switching from the outer shell to the middle shell. The switching could be provided by the following: 1) "anomalous" resistance of the outer shell plasma caused by a low plasma density of the shell as a whole [18] or local density reduction due to instability development [19]; 2) a break up of the sheath and consequent plasma flow switching due to strong nonlinear RT instability development [5] or due to perturbation near the nozzle, which could be a result of angular divergence of the gas puff [9] (a conventional gas puff looks like a truncated cone); 3) reduction in the plasma conductivity due to dense cold vapors of the electrode material near the electrode [20] or due to heat losses to the massive electrode itself, that could be more pronounced for microsecond time implosions. If the current switching from the outer to middle shell could occur, then the middle shell together with the inner shell could be considered as a double shell z-pinch driven by a faster (in comparison with 1 μs) generator. Our previous experiments with an argon double puff on the GIT-12 generator [14] at the current rise time of 300 ns (an opening switch was used) have demonstrated that K-shell yield as high as 1.1 kJ/cm can be attained when middle and inner shell diameters were 8 and 1.6 cm, respectively. Therefore, it seems quite reasonable to use approximately the same middle and inner shell radii in order to reach high argon K-shell yield.

The outer M_o, middle M_m and inner shell M_i masses were varied in the course of the experiments to find out a better K-shell radiation performance. Depending of the total puff mass the implosion time was varied from 550 to 950 ns resulting in peak current variation in the range 2.2÷3.4 MA.

The estimation of the gas mass injected into the interelectrode gap was based on the pressure measurements upstream of the nozzle critical cross-section with the use of a piezoelectric gauge. Prior to a shot, the pressure measurements were carried out. Time dependencies of the pressure were recalculated to the gas puff masses by the method described in [21].

3. Diagnostics

The diagnostics included B-dot probes and an inductive divider for the load current I and the load voltage U measurements, respectively. The time dependence of the load inductance $L(t)$ and the mean current radius $r(t)$ were estimated from relations: $L(t) \approx \int U \, dt / I$ and $L(t) = L_0 + (\mu_0 \, l/2\pi) \, ln \, (r_0/r(t))$, neglecting an active resistance contribution to the load voltage U. Here r_0 is the outer shell initial radius, L_0 is the inductance of the region between the initial outer shell position and the return current conductor, l is the z-pinch length.

The pinch image in the final stage of implosion was registered by a time-integrated pinhole camera with filters transmitted efficiently argon K-shell x-rays. The argon K-shell yield and power were measured by two PCDs. The first one (PCD1) was filtered by 3 μm Pd + 10 μm polypropylene; the second one (PCD2) was filtered by 6.35 μm Ti + 10 μm polypropylene. An x-ray diode (XRD) with aluminum cathode filtered by 2 μm kimfol + 0.2 μm aluminum was used to register softer x-rays. The main contribution to XRD response is determined by the argon L-shell radiation. The detectors sensitivities are shown in Fig. 1. The mica convex crystal spectrograph was used to observe K-shell argon spectrum.
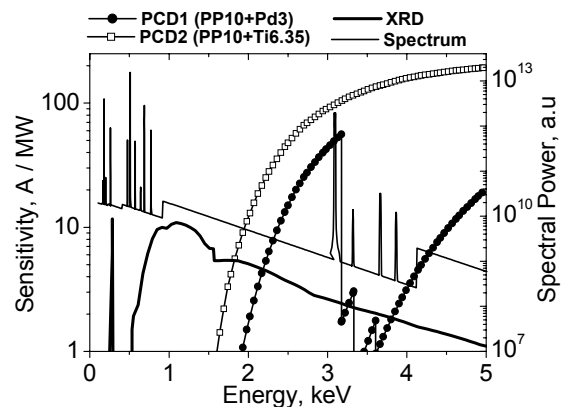

Fig. 1. The x-ray detector sensitivities and an argon spectrum calculated by collisional radiative model to show the positions of the most important K-shell and L-shell lines

4. Technique for the Plasma Electron Temperature Estimation

The diagnostic set allows estimation of the electron temperature of the plasma pinch. First, the K-shell power P_k, the time-integrated K-shell radiating pinch radius r_k and the time-integrated He-α to Ly-α line ratio can be measured. These data allow performing the electron temperature and ion density measurements in a fashion proposed in [22]. Following the

method, collisional radiative equilibrium (CRE) model calculations are performed for a uniform plasma column with the radius r_k to fit experimental values of P_k and He-α to Ly-α line ratio. The calculated ion density and electron temperature of a uniform plasma column, which provide this fit, are supposed to be some averaged parameters of the real plasma.

Second, the electron temperature can be estimated from the ratio of PCD's signals. Due to a sharp Pd L-edge cutoff at 3.17 keV, the second PCD registered net argon He-α line radiation, while the first PCD was sensitive to all K-shell lines and continuum (Fig. 1). The CRE model [23] calculations were carried out for a range of reasonable values of ion densities and plasma column radii. The ratio of He-α line power to the total K-shell radiation power was shown to be $0.85 \div 0.88$ at the electron temperature of $500 \div 900$ eV (Fig. 2).
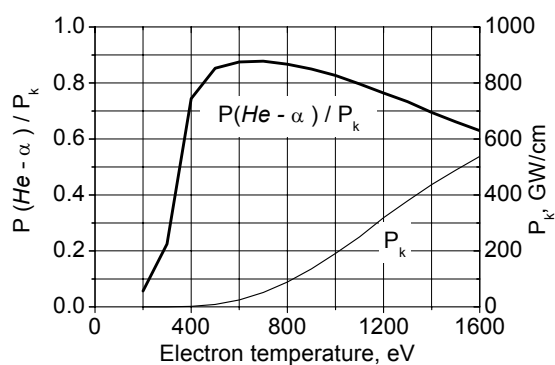

Fig.2. Argon K-shell radiation power P_k and ratio of He-α line power $P(He$-$\alpha)$ to the K-shell power P_k calculated by the CRE model at ion density of $2.4 \cdot 10^{19}$ cm^{-3} and plasma column radius of 0.1 cm

Third, the ratio of PCD response to XRD response is sensitive to the plasma electron temperature, because the PCD observes only K-shell emission, while the XRD response is conditioned mainly by the argon L-shell radiation. The responses of the XRD and PCD1 were calculated using the CRE model [23] spectrum and detector's spectral sensitivities (Fig. 1). The experimental geometry was taken into account. The calculations were performed for plasma column radii of $0.1 \div 0.3$ cm and column line masses of $50 \div 100$ μg/cm. These values were expected to be typical in the experiments. The temperature dependence of the PCD1 to XRD response ratio was calculated to be a weak function of the column radius and the line mass. The plot of the electron temperature vs ratio of PCD1 to XRD responses is shown in Fig. 3.

The calculated ratios for each temperature value were averaged, and then the temperature dependence of the detector's response ratio was approximated by an analytical expression. The expression does not introduce an error more than 15% in the temperature range of $400 \div 1000$ eV. The time dependence of the electron temperature can be determined using the ex-

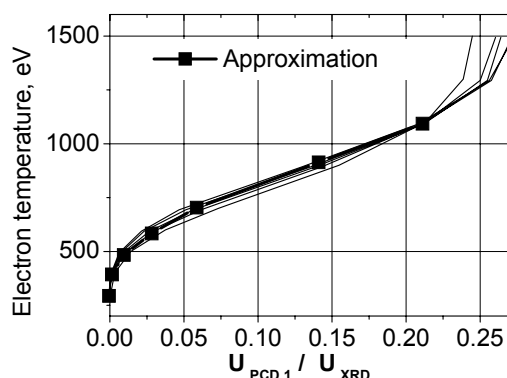perimental XRD and PCD traces and the analytical expression obtained.

Fig. 3. The electron temperature vs ratio of PCD1 to XRD responses

5. Experimental Results

The shell masses were varied in the experiments to reach a tight final pinch and to find out the better K-shell radiation performance. The final pinch with a diameter of 1.8 mm was formed at outer/middle/inner masses M_o:M_m:M_i of 50:110:50 (μg/cm) [10, 11]. The K-shell yield of 500 J/cm was registered that is approximately twice lower than the K-shell yield predicted by the two-level model [24] for a maximum current of 2.4 MA and a pinch radius of 0.1 cm.

Only weak He-α line was observed in the experimental spectrum in this shot. This did not allow application of the method [22] for electron temperature and ion density measurements. The PCD2 response was only $10 \div 15\%$ higher than PCD1 response multiplied by the ratio of PCD2 to PCD1 sensitivity for the He-α line (Fig. 4). These results give clear evidence that the electron temperature was in the range of $500 \div 900$ eV. Such electron temperature is low for efficient K-shell radiation production. Indeed, 2-fold increase in the electron temperature from 700 eV to 1400 eV results in approximately 10-fold increase in K-shell power (Fig. 3).
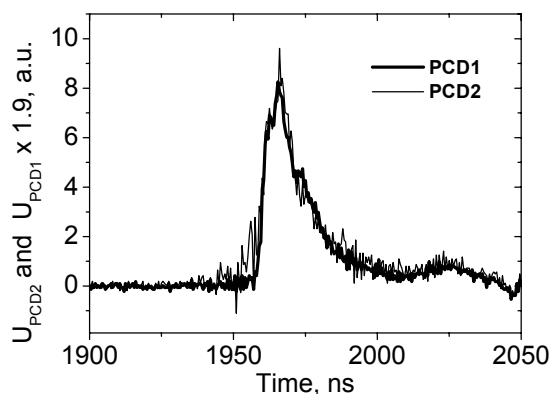

Fig. 4. The PCD1 and PCD2 traces. The PCD1 response is multiplied by a factor 1.9, that is ratio of PCD2 sensitivity to PCD1 sensitivity for argon He-α spectral line

Approximately the same electron temperature (650÷700 eV) was inferred from the ratio of PCD1 to XRD responses (Fig. 5). The electron temperature was determined in the range where the PCD1 response exceeds a threshold corresponding to 10% of its peak value. According to the CRE calculations the argon plasma ion density should be $1.8 \cdot 10^{19}$ cm^{-3} at this value of the electron temperature to provide the measured peak K-shell power of 28 GW/cm. That corresponds to the K-shell radiating mass of 30 μg/cm.
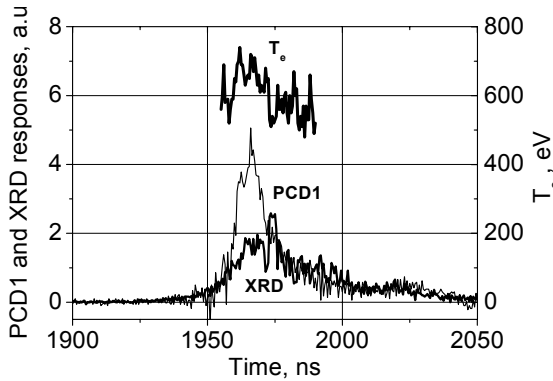

Fig. 5. PCD1 and XRD traces, the time dependence of the electron temperature T_e for the shot with the K-shell yield of 500 J/cm

The PCD1 and XRD responses, and the electron temperature T_e are shown in Fig. 6 for a shot with higher z-pinch mass. The outer/middle/inner masses M_o:M_m:M_i were 150:70:150 (μg/cm). The electron temperature does not exceed 540 eV. The low electron temperature resulted in a low K-shell yield of 100 J/cm. The absolute time scale in Fig. 4, 5 and 6 does not relate to onset of the generator current.
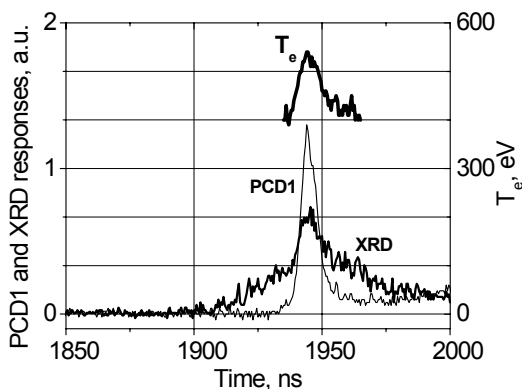

Fig. 6. PCD1 and XRD traces, the time dependence of the electron temperature T_e for the shot with the K-shell yield of 100 J/cm

The experimental traces of generator current I, load voltage U and load inductance variation $\Delta L = L(t) - L_0$ are shown in Fig. 7. The current sheath radius $r(t)$ obtained from time variation of the inductance is shown in Fig. 8 together with a z-pinch radius $r_{sp}(t)$ cal-

culated by the snow plow model for the shot with the K-shell yield of 500 J/cm. The time scale in Fig. 7 and Fig. 8 starts at the onset of the generator current.
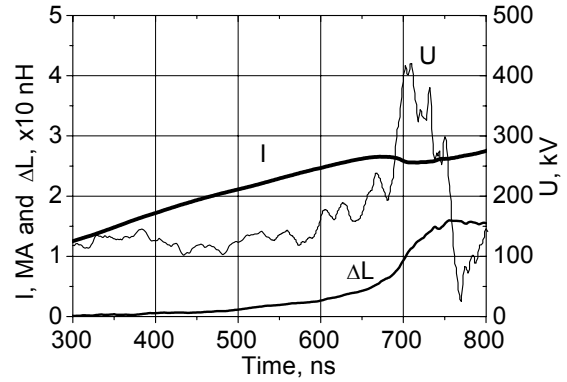

Fig. 7. Generator current I, load voltage U and load inductance variation $\Delta L = L(t) - L_0$ for the shot with the K-shell yield of 500 J/cm
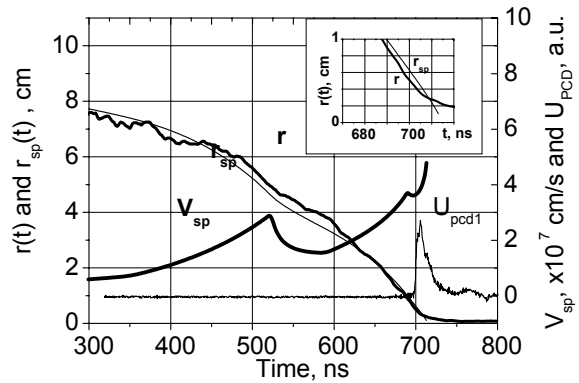

Fig. 8. Comparison of experimental current sheath radius $r(t)$ with calculated one $r_{sp}(t)$. The calculated implosion velocity V_{sp} and experimental PCD1 trace are also shown

In spite of complexity of the implosion process, the experimental radius $r(t)$ is consistent with the snow plow calculation radius until the last 5 mm of the implosion. To obtain this fit, the shell masses in the calculation were reduced only by 10% relatively to that ones measured by pressure gauges.

The most important discrepancy between $r_{sp}(t)$ and $r(t)$ is observed at the radius less 0.5 cm. The experimental dynamics evidently exhibits slowing down of the current sheath, while calculated radius $r_{sp}(t)$ continues to decrease with a rising velocity. The snow plow calculated implosion velocity reaches $4.8 \cdot 10^7$ cm/s at the 10-fold inner shell compression. This velocity value corresponds to the kinetic energy per ion of 1.3 E_{min}, that should provide plasma ionization into K-shell and efficient excitation and emission of the K-shell electrons. The maximum velocity inferred from the experimental radius $r(t)$ does not exceed $3.5 \cdot 10^7$ cm/s and kinetic energy per ion is significantly lower than E_{min}.

378

6. Discussion and Conclusion Remarks

The slowing down of the current sheath was observed in microsecond implosion time experiments at the current level of 7÷12 MA [3]. In those experiments carried out with a thin aluminum foil mounted at the initial radius of 7 cm, the shell deceleration became evident at the radius of 1.5 cm. The diameter of the plasma pinch in the spectral range above 1 keV was measured to be 0.5÷2 cm. X-ray yield as low as 0.5÷2 kJ/cm was obtained in the spectral range $h\nu \geq 1$ keV.

The plasma deceleration in the final implosion stage is mostly determined by the high amplitude instabilities developing in the course of the implosion. Both the instability development and electrode ablation can cause a residual plasma breakdown and formation of a secondary current path at the radius of few centimeters [3]. This current shunting can reduce the energy delivered to the plasma pinch.

The multiple gas puff shell z-pinch exhibits the slowing down at the smaller radius of 0.5 cm, perhaps due to higher implosion stability. Nevertheless, the observed sheath deceleration still limits the energy delivery to the plasma pinch. As a result, the electron temperature is rather low (≈ 700 eV) that leads to the low argon K-shell yield of 500 J/cm, in spite of the fact that a tight K-shell radiating pinch with the diameter of 0.18 cm is obtained.

Thus, the experimental results have shown that the final implosion velocity was overestimated in the preliminary snow plow calculations, which were used to choose the multiple shell z-pinch initial radii. It seems reasonable to increase the initial radius of the outer shell by $\approx 20\div30\%$ to provide higher final velocity and higher electron temperature of the plasma pinch. That, in its turn, should provide higher argon K-shell radiation yields at the microsecond implosion time regime.

References

[1] N.R. Pereira and J. Davis, J. Appl. Phys. **64**, R1 (1988).

[2] K.G. Whitney, J.W. Thornhill, J.P. Apruzese, and J. Davis, J. Appl. Phys. **67**, 1725 (1990).

[3] W.L. Baker, M.C. Clark, J.H. Degnan et al., J. Appl. Phys. **49**, 4694 (1978).

[4] J.H. Degnan, R.E. Reinovsky, D.L. Honea, and R.D. Bengston, J. Appl. Phys. **52**, 6550 (1981).

[5] T.W. Hussey, N.F. Roderick, and D.A. Kloc, J. Appl. Phys. **51**, 1452 (1980).

[6] F.L. Cochran, J. Davis, and A.L Velikovich, Phys. of Plasmas **2**, 2765 (1995).

[7] P. Sincerny, S. Wong, V. Buck et al., *in: Proc. 5th Pulsed Power Conf.*, 1985, pp. 701–703.

[8] R.B. Baksht, A.V. Lutchinsky, and A.V. Fedunin. Rus. J. Tech. Physics **62**, 145 (1992).

[9] S.A. Chaikovsky and S.A. Sorokin, Rus. Plasma Physics **27**, 1003 (2001).

[10] A.V. Shislov et al., see these proceedings.

[11] S.A. Chaikovsky et al., see these proceedings.

[12] C. Deeney, P.D. LePell, B.H. Failor et al., J. Appl. Phys. **75**, 2781 (1994).

[13] S.A. Sorokin and S.A. Chaikovsky, Rus. Plasma Physics **22**, 992 (1996).

[14] A.V. Shishlov, R.B. Baksht, S.A. Chaikovsky et al., *in Proc. 5th Intern. Conf. on Dense Z-pinches*, 2002, pp. 117–122.

[15] S.M. Gol'berg, A.L. Velikovich, *in Proc. 3rd Intern. Conf. on Dense Z-pinches*, 1993, pp. 42–50.

[16] A.L. Velikovich, F.L. Cochran, and J. Davis, Phys. Rev. Lett. **77**, 853 (1996).

[17] J.H. Hammer, J.L. Eddleman, M. Tabak et al., *in: Proc. 11th Intern. Conf. on High Power Particle Beams,* 1996, pp. 721–724.

[18] A.V. Branitsky, S.A. Dan'ko, A.V. Gerusov et al., Rus. Plasma Physics **22**, 307 (1996).

[19] A. Chuvatin, P. Choi, and B. Etlicher, Phys. Rev. Lett. **76**, 2282 (1996).

[20] S.V. Bazdenkov, K.G. Gureev, N.V. Fillipov, and T.N. Fillipova, Rus. JETP Lett. **18**, 199 (1973).

[21] A.Yu. Labetsky, A.G. Rousskikh, A.V. Fedunin, and A.V. Shishlov, Rus. Phys. Jour. **42**, 1047 (1999).

[22] J.P. Apruzese, K.G. Whitney, J. Davis, and P.C. Kepple, JQSRT **57**, 41 (1997).

[23] V.I. Oreshkin, Rus. Preprint of TSC **5** (1991).

[24] D. Mosher, N. Qi, and M. Krishnan, IEEE Trans. Plasma Sci. **26**, 1052 (1998).